Supplementary Information

Understanding Charge Storage in Nb_2CT_x MXene as Anode Material for Lithium Ion Batteries

Renfei Cheng[a,b], Tao Hu[c], Zuohua Wang[d], Jinxing Yang[a,b], Ruqiao Dai[a,b], Weizhen Wang[a], Cong Cui[a,b], Yan Liang[a], Chao Zhang[a], Cuiyu Li[e], Hailong Wang[f], Hongxia Lu[f], Zhiqing Yang[a], Hongwang Zhang[d], Xiaohui Wang*[a]

[a] Shenyang National Laboratory for Materials Science, Institute of Metal Research, Chinese Academy of Sciences, Shenyang 110016, China
[b] School of Materials Science and Engineering, University of Science and Technology of China, Shenyang 110016, China
[c] Institute of Materials Science and Devices, Suzhou University of Science and Technology, Suzhou 215009, China
[d] National Engineering Research Center for Equipment and Technology of Cold Strip Rolling, College of Mechanical Engineering, Yanshan University, Qinhuangdao 066004, China
[e] Advanced Computing East China Sub-center, Suma Technology Company Limited, Kunshan 215300, China
[f] School of Materials Science and Engineering, Zhengzhou University, Zhengzhou 450001, China

*Corresponding author
***E-mail**:* wang@ imr.ac.cn (X. Wang)

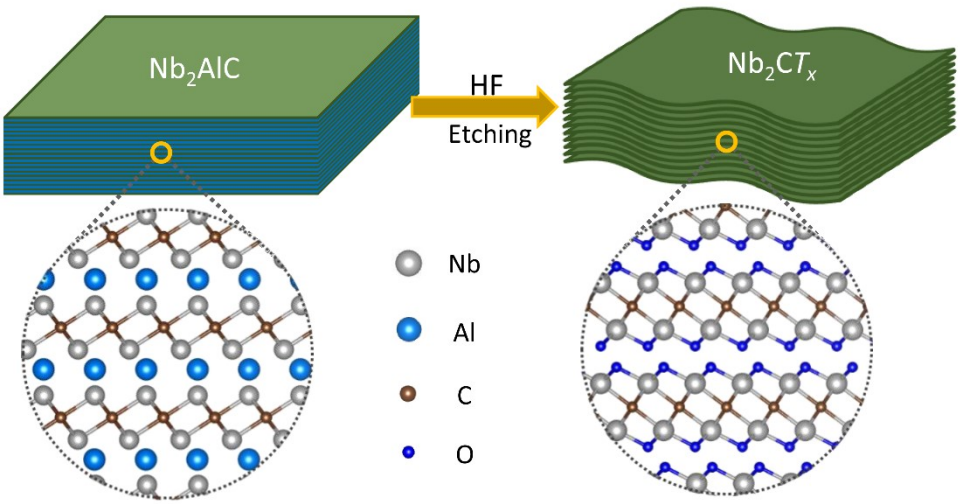

Fig. S1 Schematic diagram for synthesis of multilayer Nb_2CT_x MXene.

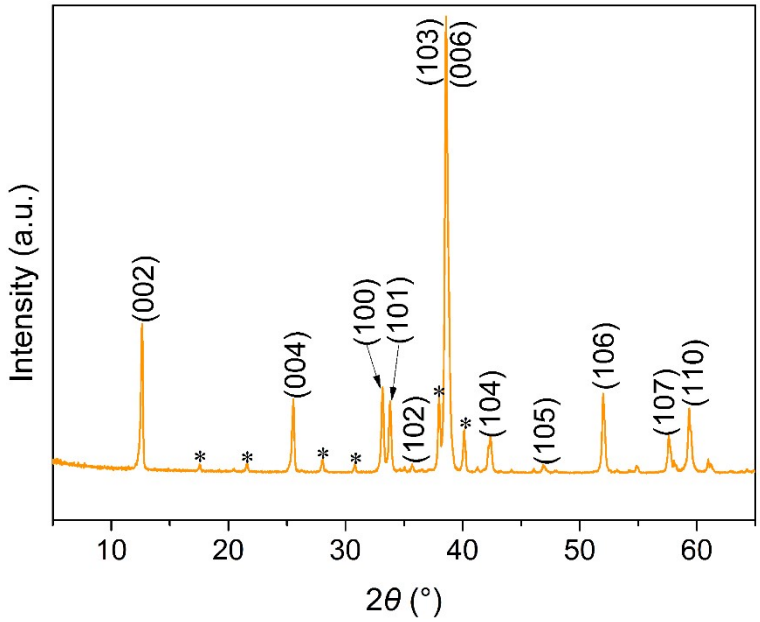

Fig. S2 Powder XRD pattern of as-prepared Nb_2AlC. The asterisks indicate Nb_3Al_2C as a secondary phase in the as-prepared Nb_2AlC MAX phase.

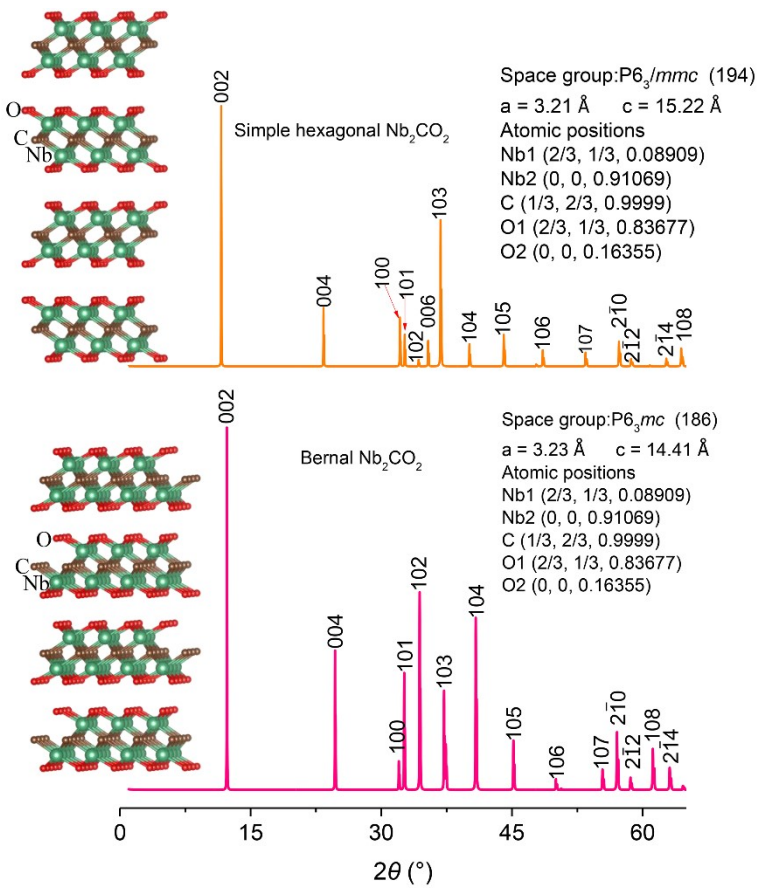

Fig. S3 Simulated XRD patterns of simple hexagonal and Bernal stacked Nb_2CO_2.

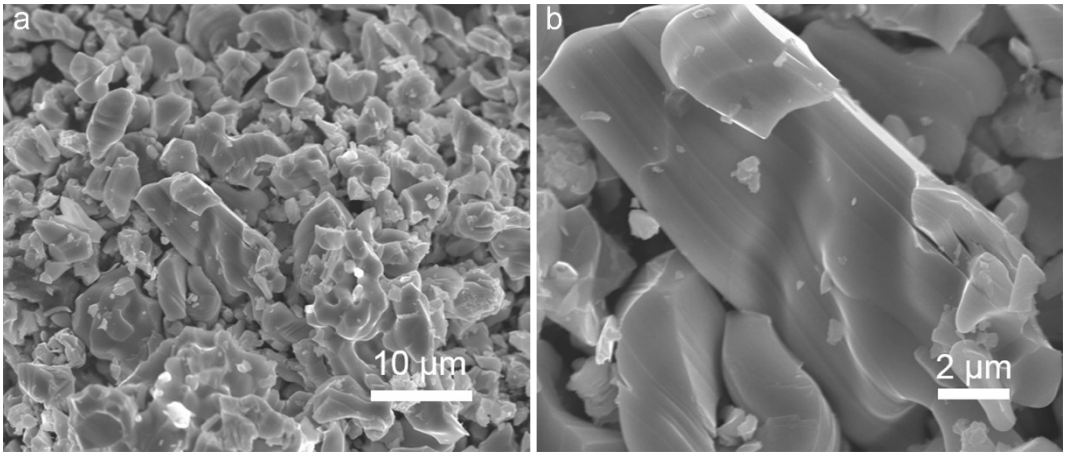

Fig. S4 SEM images of Nb_2AlC with different magnifications.

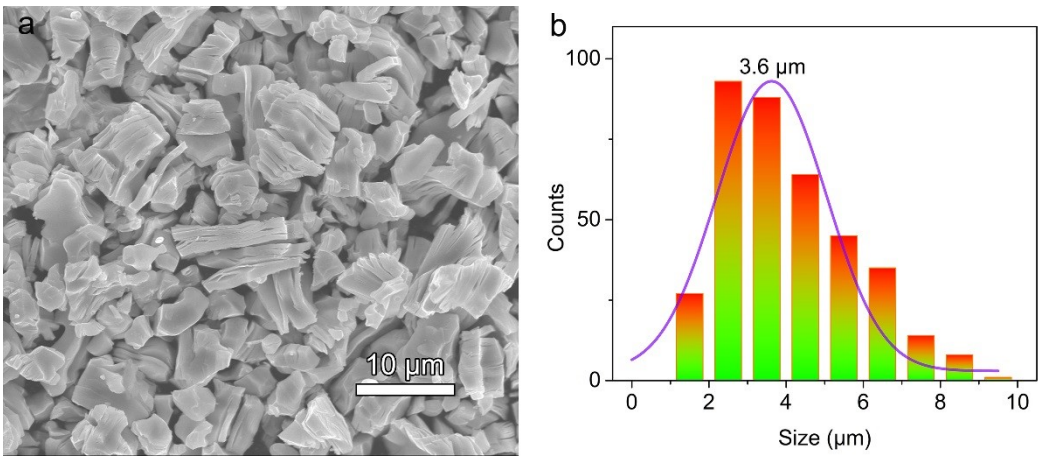

Fig. S5 (a) SEM image, and (b) statistical size distribution histogram of Nb_2CT_x.

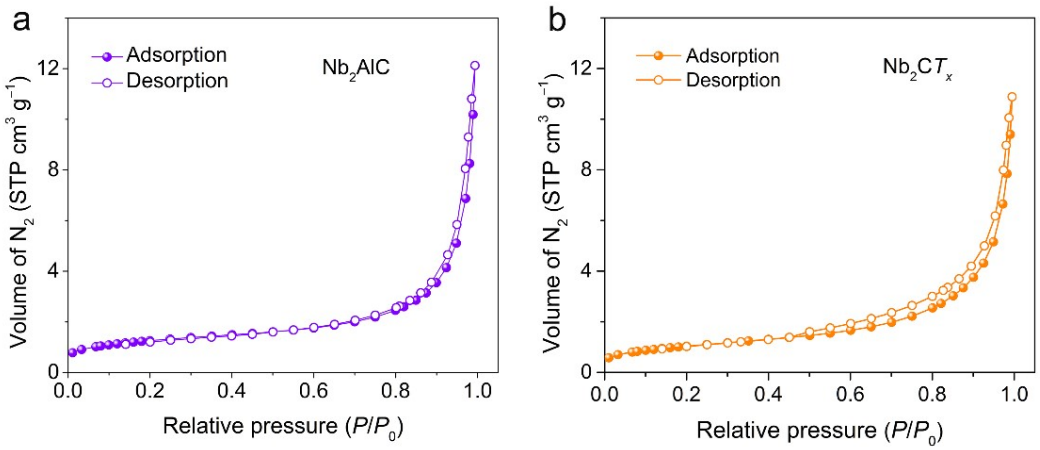

Fig. S6 Nitrogen adsorption/desorption isotherms of (a) Nb_2AlC and (b) Nb_2CT_x. The BET specific surface areas of Nb_2AlC and Nb_2CT_x are 4.5 and 3.8 m^2 g^{-1}, respectively.

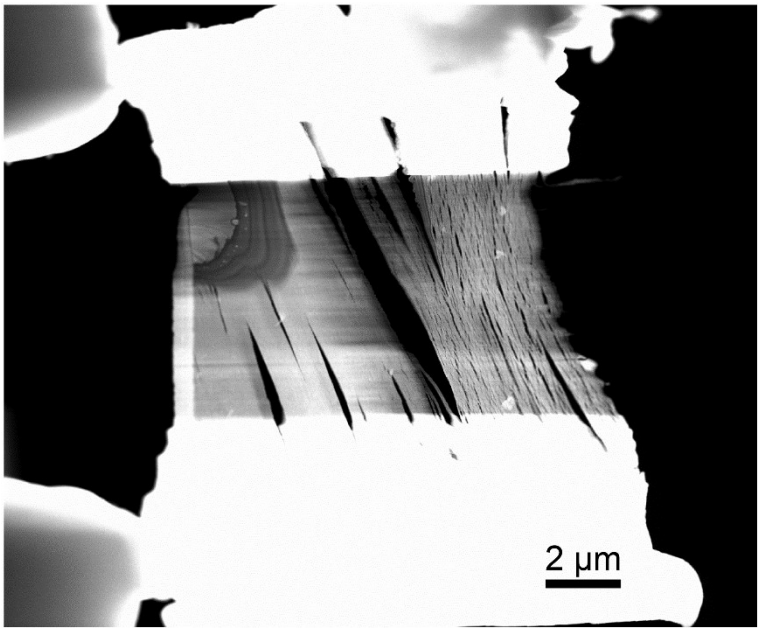

Fig. S7 Cross-sectional microstructure of Nb_2CT_x.

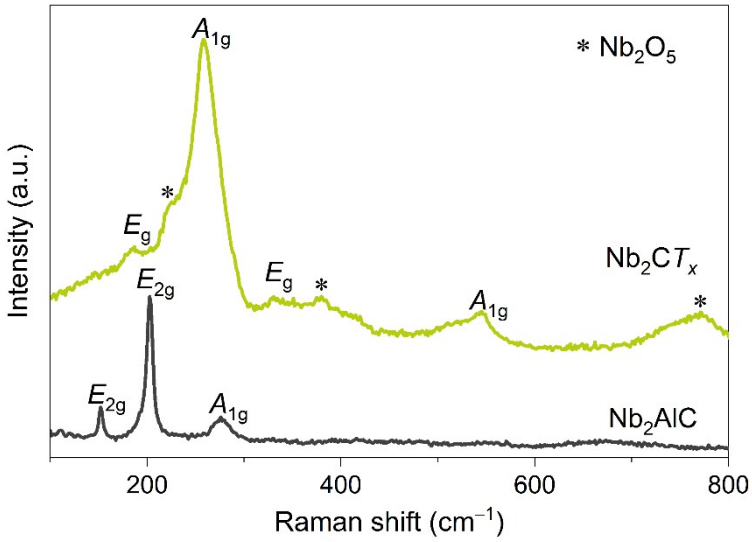

Fig. S8 Raman spectra of Nb_2AlC MAX phase and Nb_2CT_x MXene. The asterisks indicate the Raman bands of Nb_2O_5 existed on the surface of Nb_2CT_x.

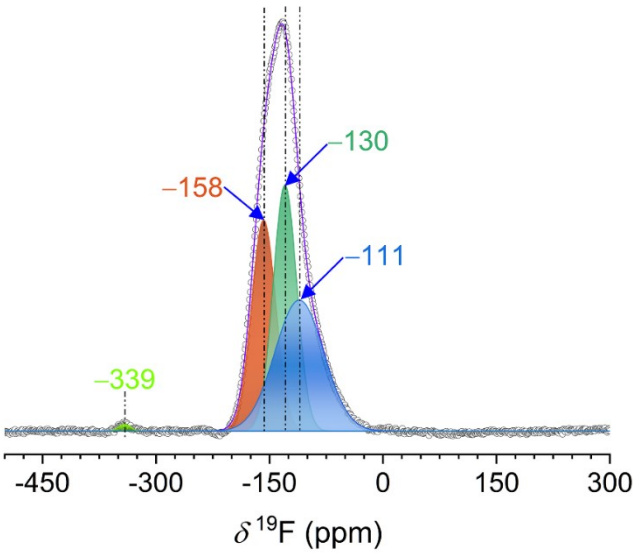

Fig. S9 ^{19}F NMR spectrum of Nb_2CT_x collected at 14 T under 12 kHz magic-angle spinning.

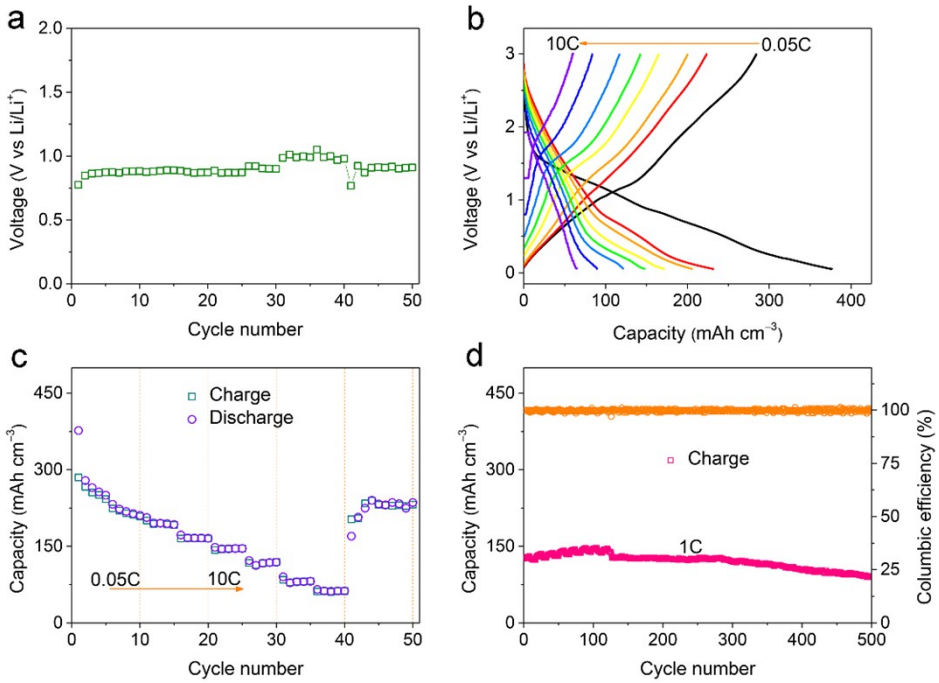

Fig. S10 (a) The operating voltage of Nb_2CT_x at different cycle. (We evaluated the average voltage of Nb_2CT_x using the equation: $E = Q\ V_{op}$, where E is energy density, V_{op} is operating voltage, and Q is reversible capacity.[1]) (b) Charge/discharge curves of Nb_2CT_x at various rates. (c) Rate performance of Nb_2CT_x at various rates. (d) Long-term cycling performance of Nb_2CT_x at a rate of 1C.

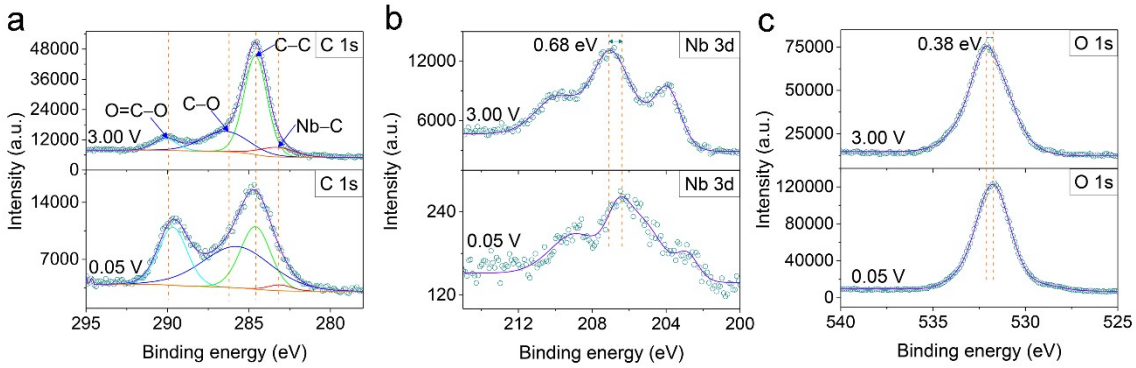

Fig. S11 Ex situ XPS high resolution spectra of C 1s, Nb 3d, and O 1s at state of full lithiation (0.05 V) and full delithiation (3.0 V).

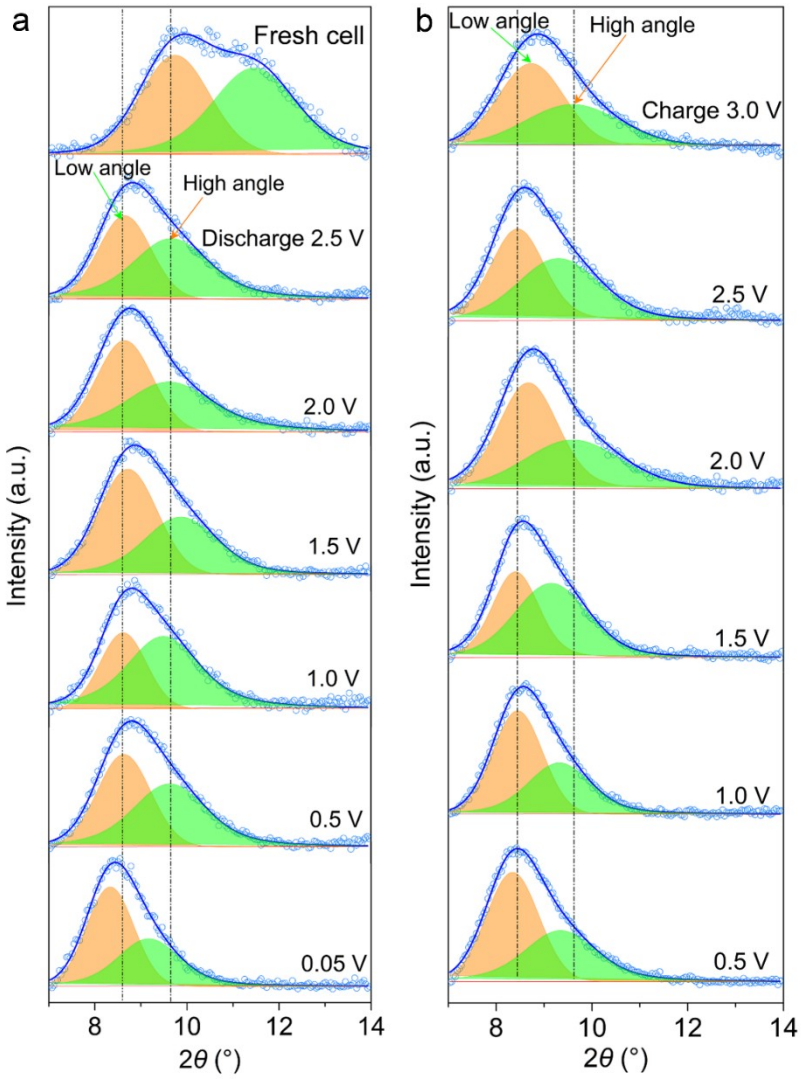

Fig. S12 Cell voltage dependence of XRD patterns of Nb_2CT_x. Note that the peaks are fitted with Voigt function.

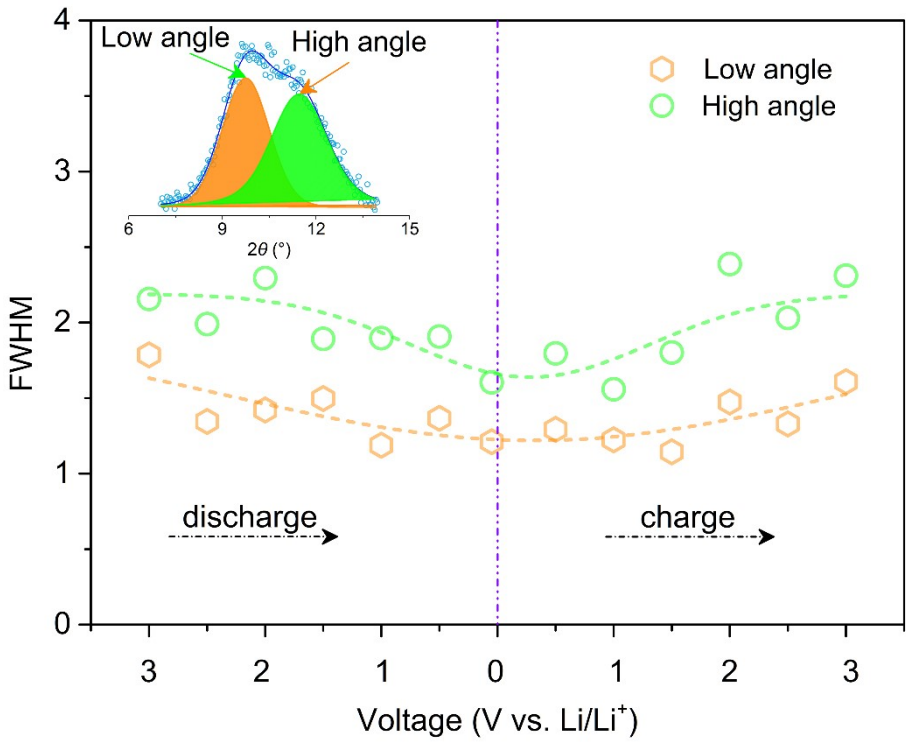

Fig. S13 Change of FWHM for Nb_2CO_x during the discharge and charge process. FWHM is the abbreviation of full width at half maximum.

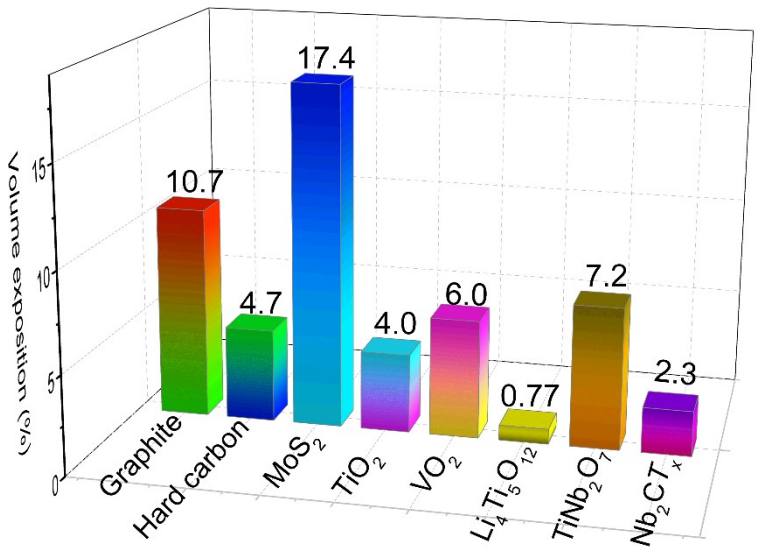

Fig. S14 Comparison of the volume expansion of the Nb_2CT_x with previously reported intercalation anode materials[2-8].

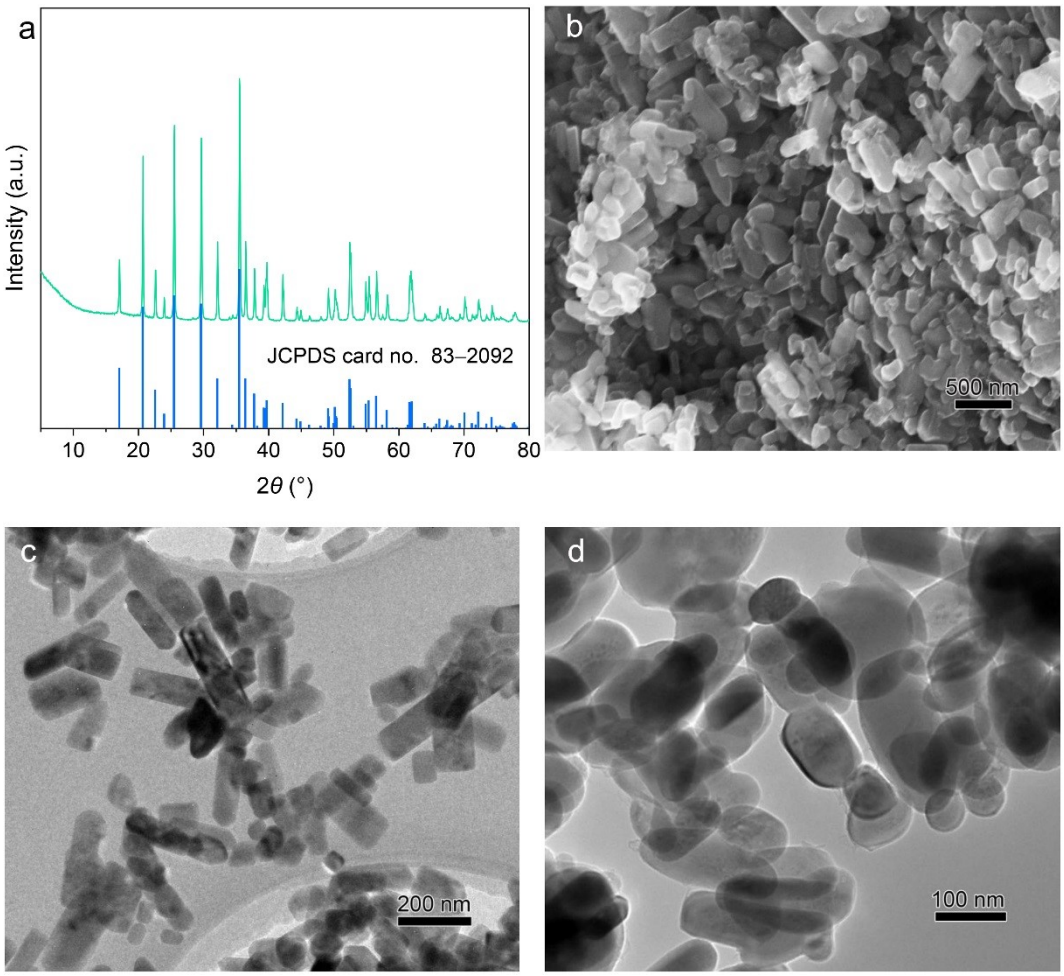

Fig. S15 (a) XRD pattern of the as-prepared $LiFePO_4$ product. SEM image (b), TEM images (c, d) of $LiFePO_4$/C material.

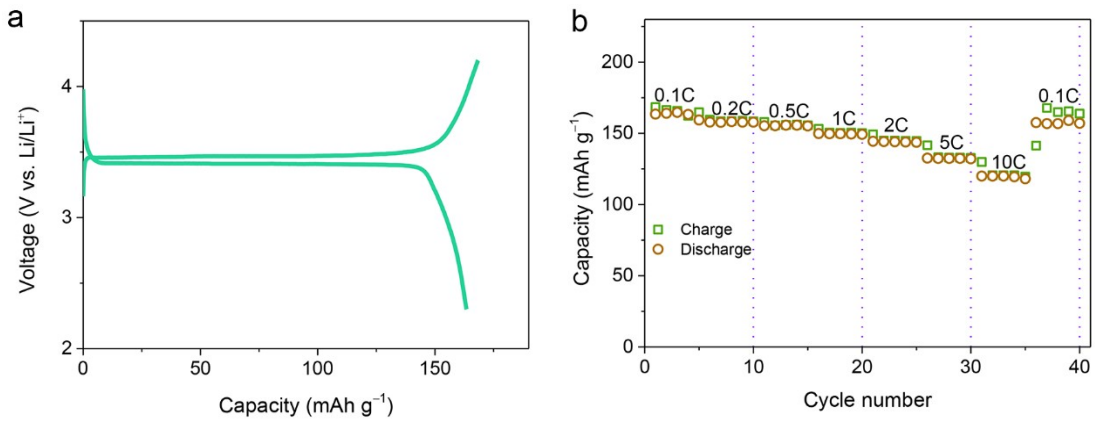

Fig. S16 (a) First charge and discharge profiles of the half cell with $LiFePO_4$ cathode composites at a rate of 0.1 C (1C = 170 mAh g^{-1}). (b) Rate performance of the $LiFePO_4$ cathode in the half cell.

Table S1. Nb 3d core level peak analyses. Each peak corresponds to a specific type of niobium: Nb–C, C–Nb–O, or Nb–O. Nb 3d core level was fitted with a fixed area ratio of 3:2 for all Nb 3d5/2–Nb 3d3/2 and doublet separation of 2.8 eV for Nb–C, 2.8 eV for C–Nb–O, and 2.8 eV for Nb–O.

Sputtering time	Fraction (%)		
	Nb–C	C–Nb–O	Nb–O
	202.7±0.1 eV	206.0±0.1 eV	207.0 eV
0 s	39.8±4.9	40.1±4.9	20.1±4.9
60 s	72.6±6.9	27.4±6.9	–
120 s	77.1±7.9	22.9±7.9	–

Table S2. O 1s core level peak analyses. Each peak corresponds to a specific type of oxygen: Nb–O, C–Nb–O or H_2O_{ads}.

Sputtering time	Fraction (%)			
	Nb–O	C–Nb–O	H_2O_{ads}	C–O
	530.1 eV	531.2±0.2 eV	532.5±0.2 eV	533.3±0.1 eV
0 s	35.4±3.3	39.0±3.3	11.4±3.3	14.2±3.3
60 s	–	84.8±4.7	6.8±4.7	8.4±4.7
120 s	–	75.4±4.1	15.4±4.1	9.2±4.1

Table S3. C 1s core level peak analyses. Each peak corresponds to a specific type of carbon: Nb–C, C–C, C–O or O–C=O.

Sputtering time	Fraction (%)			
	Nb–C	C–C	C–O	O–C=O
	282.4±0.1 eV	284.6	285.5±0.1 eV	288.4 eV
0 s	10.6±4.0	58.0±4.0	13.8±4.0	17.6±4.0
60 s	23.4±3.4	60.5±3.4	16.1±3.4	–
120 s	27.3±3.7	72.7±3.7	–	–

Table S4. Summary of atomic composition in the Nb_2CT_x.

Element	Atomic fraction (%)	Error (%)
Nb	34.67	7.14
C	17.73	2.99
O	39.37	10.21
F	7.64	1.98
Al	0.59	0.15

Table S5. Bader charge of the elements in $Nb_2CO_2Li_2$ and Nb_2CT_x with different terminated groups.

	Bader charge					
	Nb	C	O	Li	F	H
$Nb_2CO_2Li_2$	1.59	−1.77	−1.55	0.84	–	–
Nb_2CF_2	1.65	−1.80	–	–	−0.75	–
$Nb_2C(OH)_2$	1.66	−1.82	−1.31	–	–	0.55
Nb_2CO_2	2.04	−1.75	−1.16	–	–	–

References

1 Y. Tang, Y. Zhang, W. Li, B. Ma and X. Chen, *Chem. Soc. Rev.*, 2015, **44**, 5926-5940.

2 M. Winter, J. O. Besenhard, M. E. Spahr and P. Novák, *Adv. Mater.*, 1998, **10**, 725-763.

3 A. Agrawal, K. Biswas, S. K. Srivastava and S. Ghosh, *J. Solid State Electrochem.*, 2018, **22**, 3443-3455.

4 C. D. Quilty, L. M. Housel, D. C. Bock, M. R. Dunkin, L. Wang, D. M. Lutz, A. Abraham, A. M. Bruck, E. S. Takeuchi, K. J. Takeuchi and A. C. Marschilok, *ACS Appl. Energy Mater.*, 2019, **2**, 7635-7646.

5 R. van de Krol, A. Goossens and E. A. Meulenkamp, *J. Electrochem. Soc.*, 1999, **146**, 3150-3154.

6 Q. Liu, G. Tan, P. Wang, S. C. Abeyweera, D. Zhang, Y. Rong, Y. A.Wu, J. Lu, C.-J. Sun, Y. Ren, Y. Liu, R. T. Muehleisen, L. B. Guzowski, J. Li, X. Xiao and Y. Sun, *Nano Energy*, 2017, **36**, 197-205.

7 P. C. Tsai, W. D. Hsu and S. K. Lin, *J. Electrochem. Soc.*, 2014, **161**, A439-A444.

8 B. Guo, X. Yu, X.-G. Sun, M. Chi, Z. A. Qiao, J. Liu, Y. S. Hu, X. Q. Yang, J. B. Goodenough and S. Dai, *Energy Environ. Sci.*, 2014, **7**, 2220-2226.